Behavior of the contacts of quantum Hall effect devices at high currents

Cite as: Journal of Applied Physics **96**, 404 (2004); https://doi.org/10.1063/1.1748853
Submitted: 21 October 2003 . Accepted: 25 March 2004 . Published Online: 17 June 2004

Y. M. Meziani, C. Chaubet, S. Bonifacie, A. Raymond, W. Poirier, and F. Piquemal

Behavior of the contacts of quantum Hall effect devices at high currents

Y. M. Meziani,[a] C. Chaubet, S. Bonifacie, and A. Raymond
Groupe d'Etude des Semiconducteurs, UMR CNRS 5650, Université Montpellier II, 34095 Montpellier Cedex France

W. Poirier and F. Piquemal
Bureau National de Métrologie, Laboratoire National d'Essais (BNM-LNE) 33, Avenue du Général Leclerc 92260 Fontenay aux Roses, France

(Received 21 October 2003; accepted 25 March 2004)

We have analyzed the behavior of contacts of quantum Hall effect devices while increasing the current through the sample. Experiments have been performed in the $i=2$ plateau, which is used in all metrological measurements of the von Klitzing constant R_K, before the onset of dissipation. Using only electrical measurements, we show that a high electric field zone appears in the vicinity of the current contact which injects the electrons in the two-dimensional electron gas, when the current is increased. This heating phenomenon develops in the region close to the source, increases the electronic temperature in the sample, and limits the precision in the measurement of R_K. We have studied several samples of different width, using a well-defined configuration for the measurements. It is observed that the threshold current for the onset of the voltage drop across the contact increases with the width of the Hall bar. Consequences for high precision measurements are discussed in terms of experimental protocol and of contact's geometry. © *2004 American Institute of Physics.* [DOI: 10.1063/1.1748853]

I. INTRODUCTION

The Hall resistance R_H of a two-dimensional electron gas is quantized at low temperature when the filling factor ν of the Landau levels is near an integer.[1–3] At the same time, the longitudinal resistance R_{xx} of Hall-bar conductors vanishes as long as the current does not exceed a critical value.[1–4] The plateau $i=2$ is used in the metrological applications of the quantum Hall effect (QHE) to provide a very reproducible resistance standard. Typically, $R_H(i=2)$ does not deviate from $R_K/2$ by more than one part in 10^9 (relative value) if the Hall sample used fulfills certain conditions. The von Klitzing constant R_K is expected to correspond to the ratio h/e^2. The recommanded value of R_K for metrology use is 25 812.807; Ω with a relative uncertainty of one part in 10^7.[5] The amplitude of the current which circulates across the sample must be limited to guarantee the accuracy of the measurement. Indeed, the onset of the longitudinal resistance R_{xx} while increasing the current which is known as the breakdown of the quantum Hall effect,[6–8] destroys the total quantization of the system and prevents the measurement from being feasible. But in reality, far before the breakdown, another phenomenon affects the accuracy of the measurement of R_K. It is due to a linear relationship between R_H and R_{xx}.[8,9] Then, even a very small increase of the longitudinal resistance R_{xx} can cause a deviation of R_H from its expected value $R_K/2$. Typically, the deviation does not exceed one part in 10^9 in relative value only if the longitudinal resistance stays below 100 $\mu\Omega$. This is the reason why the metrological measurements are performed using current intensities which are always smaller than the breakdown current (see Refs. 7 and 8).

Our article reports on this limitation of the current in high precisison measurements. We show that under well-defined configurations for the measurement, one can obtain the threshold current by measuring the voltage drop across the contact. Indeed, well before the abrupt onset of dissipation, i.e., in the prebreakdown regime, the onset of the voltage drop across the contact heralds the slightest increase of R_{xx}. Therefore, the voltage drop across the contact allows one to define the threshold current for metrological measurements. We have also measured and compared the threshold currents for samples of different widths. Conclusions are drawn concerning the width of the current contacts in metrological samples, and the configuration allowing the most precise measurement for both metrological purposes and experiments on the breakdown of the quantum Hall effect.

This article is organized as follows. We present the GaAlAs/GaAs samples in Sec. II. Then in Sec. III, we detail our experimental protocol used to measure the voltage drop across the contact and the longitudinal voltage. Indeed it was important to identify the configuration that allows a general understanding of the injection mechanisms for any class of samples. Section IV is devoted to the presentation of the experimental data which illustrates the primary importance of contacts in high precision measurements. Finally in Sec. V, we discuss why these results should encourage the community of high precisison measurement to optimize the geometry of the contacts, and might encourage the community of the QHE breakdown to clearly define the configurations for their measurements.

[a]Electronic mail: yahya@ges.univ-montp2.fr

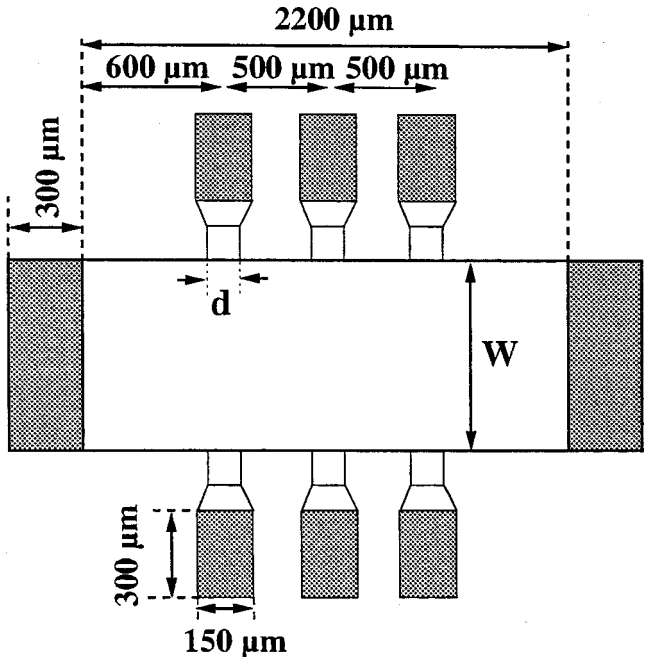

FIG. 1. The Hall bars are composed by a main channel whose width W ranges from 200 to 1600 μm. Two current contacts are used as a drain and a source. Six other lateral contacts which are smaller are used to measure the voltage drops. Their channel width d ranges from 5 to 150 μm as resumed in Table I.

II. SAMPLES

We have investigated four series of samples (PL173, PL174, PL175, and LEP514) which were all processed in the same Philips Laboratory (PL, formerly LEP) in Limeil Brévannes. They are GaAs/GaAlAs heterojunctions grown on 3 in. wafers by the metal organic chemical vapor deposition technique. This technique allows us to obtain a good homogeneity of the electronic density over a large scale. Starting from the substrate, a 600-nm-thick undoped GaAs buffer layer is first deposited. It is followed by an undoped $Al_{0.28}Ga_{0.72}As$ spacer layer whose thickness is, respectively, 22 and 14.5 nm for PL175 and PL173 heterostructures. Then a 40-nm-thick $10^{18}\,cm^{-3}$ Si-doped $Al_xGa_{1-x}As$ layer is deposited, with a gradual decrease of x from 0.28 to 0 for PL175 and homogeneous $x=0.28$ value for PL173. The two other types of samples, PL174 and LEP514, have similar layers.[8,10,11] Finally, a n-type 12 nm GaAs cap layer covers the heterostructure to improve the quality of ohmic contacts. After the realization of the 300-nm-thick delimiting mesa, the AuGeNi ohmic contacts are evaporated and then annealed at 450 °C.

All samples were processed into a Hall bar. They have six independent lateral contacts in addition to the source and drain contacts, as described in Fig. 1. LEP514, previously studied in a European project,[11] has only one size (see Table I). The other samples are fabricated with different sizes. The Hall bar width W of the PL175 sample (respectively, PL173) ranges from 200 to 800 μm (respectively, 1600). These two series allowed us to study the influence of the channel width on the injection of electrons. The samples PL174 were processed in a 400 μm wide Hall bar. The channel width d of the lateral contact for this series ranges from 5 to 150 μm.

TABLE I. Samples characteristics (ν is the filling factor of the Landau levels).

WAFER	N_s ($10^{15}\,m^{-2}$)	μ ($m^2/V\,s$)	$B(\nu=2)$ (T)	Width W (μm)	Length d (μm)
PL173	3.3	50	6.8	200, 400, and 1600	50
PL174	4.5	50	9.4	400	5, 50, and 150
PL175	4.3	42.5	9	200, 400, and 800	50
LEP514	5.1	30	10.7	400	50

The samples were connected on TO-8 ceramic holders having 12 contacts and featuring leakage resistances between pins higher than $10^{13}\,\Omega$ at room temperature. These ceramics were mounted on a sample holder whose wires are 0.2 mm diameter constantan and placed inside a variable temperature insert, in a 16 T superconducting magnet. All experiments were performed at 1.5 and 4.2 K.

III. CONFIGURATION FOR HIGH PRECISION MEASUREMENTS

A. Voltage drops near the contacts in the QHE regime

All the measurements below have been performed at the $i=2$ plateau. In the QHE regime, the magnetic field B strongly bends the potential profile. As a consequence, if a constant current I is applied between the source and drain contacts, all electrons enter the Hall bar by one corner on the source side and leave by the opposite corner on the drain side[12–14] (see Fig. 2). The existence of electron entry and exit corners was observed by Klass *et al.*[12] and later by Kawano and Komiyama.[15] These corners are high electric field spots created by a concentration of the Hall potential over a very narrow region of characteristic length 10 μm. This is illustrated in Fig. 2, where the entry and exit corners are clearly labeled. The Hall voltage V_H can be measured across those "hot spots" as shown in Fig. 2. One can measure the resistance of the current contact through the other corners of the sample (corners labeled 1 and 2 in same figure).

Voltage drops at the vicinity of the current contact are obtained using a four-wire measurement. Two wires are used to inject the current in the Hall bar and two other wires

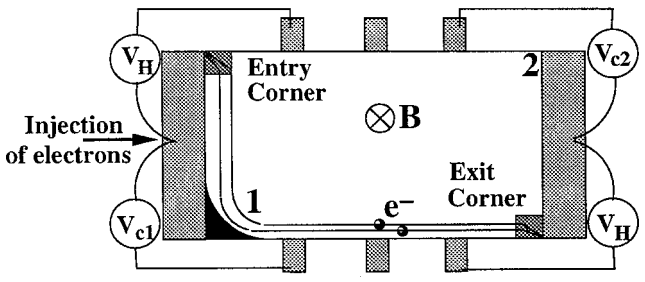

FIG. 2. Illustration of electron motion in the QHE regime and of the voltage drops in Hall bars. The resistance contact is measured in the opposite corners of the electron entry and exit corner referenced as points 1 and 2. The Hall voltage V_H appears symmetrically in the sample. The dark zone at point "1" represents the "additional heated region."

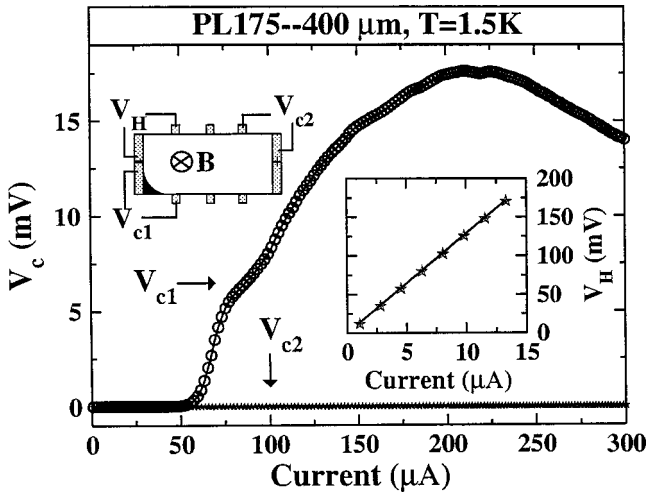

FIG. 3. Measurement of V_{c1}, V_{c2}, and V_H for sample PL175 at the $i=2$ plateau. Electrons are injected from the left contact. In the inset, V_H increases linearly with the current. V_{c1} exhibits an abrupt onset of dissipation while V_{c2} is stuck at zero. The heating process occurs only near the current contact which injects the electrons in the 2DEG. The dark zone represents the "additional heated region."

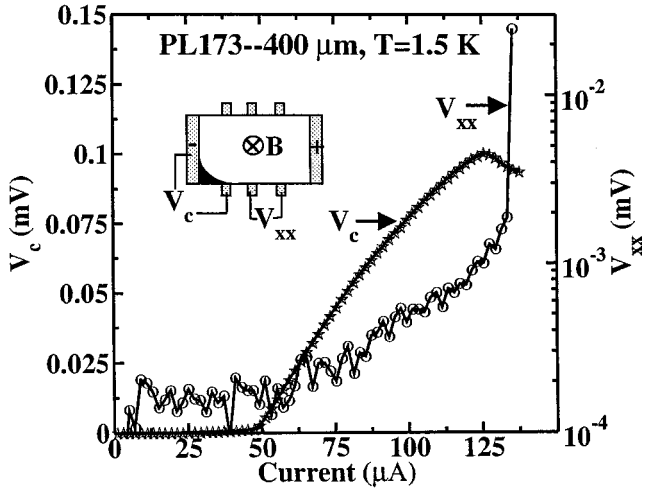

FIG. 4. Measurement of V_{xx} (○) and V_c (★) for sample PL173 with Hall bar width 400 μm. V_{xx} scale is logarithmic. The configuration of the measurements is shown in the inset.

enable the measure of the voltage drop between one current contact and one adjacent lateral contact. The Hall voltage $V_H=R_H\times I$ may be measured between the two contacts surrounding either the entry or the exit corner (see inset of Fig. 3). More surprising are the behaviors of the other corners labeled 1 and 2 which differ from one another (Fig. 2). This is obvious in Fig. 3 where we report the curves $V_{c1}(I)$ and $V_{c2}(I)$ for sample PL175. The curve $V_{c1}(I)$ exhibits a steep increase at $I=50\,\mu$m, while $V_{c2}(I)$ remains stuck at zero. V_{c2} becomes finite only for higher current values corresponding to the so-called breakdown regime. Since we are only interested in the onset of dissipation, we will only focus on the contact whose resistance increases the first. Then, V_{c1} will be denoted V_c, V_{c2} being meaningless.

B. Injection of hot electrons

The abrupt increase of the contact resistance V_c/I is the signature of a heating process near the contact which injects the electrons in the two dimensional election gas (2DEG). Recently it has been shown that a high electric field provokes strong momentum exchange that causes the resistivity to increase in this regime.[16] High electric field enhances the inter- and intra-Landau level scatterings assisted by acoustical phonons,[17,18] and induces a nonequilibrium electronic population in the vicinity of the contact which injects the electrons in the sample (the source).

We stress that the observation of Landau emission made by Kawano and Komiyama[15] and Kawano, Hisanaga, and Komiyama[19] using far infra red experiments, is another signature of the same heating phenomenon. It consists in an additional cyclotron emission (CE) signal observed in the vicinity of the source contact when the current is increased. The authors observed that at low-level current for which the two terminal resistance is still quantized, the cyclotron emission is observed at the electron entry and exit corners formed between the metallic current contacts and the two-dimensional electron gas. But when the current is increased, an additional CE signal is observed in the vicinity of the source contact. It is well known that high electric fields induces Landau emission.[17] Thus, our experimental observations and those made by Kawano and Komiyama and Kawano, Hisanaga, and Komiyama can both be explained by the presence of high electric fields in the region close to the source.

The first physical consequence of such a high electric field zone is the increase of the electronic temperature.[17] Afterward, the hot electrons are injected into the sample because of their drift velocity $V_d=E_H/B$ (E_H is the Hall electric field). As explained in the bootstrap electron heating model (BSEH),[20–25] the electrons propagate their hot temperature. It is then appropriate to measure the longitudinal voltage drops along the electrons paths. The distance between the current contact and the first voltage probe is 600 μm (see Fig. 1) which is much larger than the minimum length which is necessary to equilibrate the electronic temperature according to the BSEH model. Komiyama *et al.*[22] have measured a minimum length of 130 μm in the $i=2$ plateau to observe a steady state behavior of the longitudinal voltages.

The correlation between the heating phenomenon near the contact and the transport properties of the sample far from the contact is illustrated in Fig. 4. We have measured simultaneously the voltage drop V_c and the longitudinal voltage V_{xx}, using the configuration shown in the inset. We plotted the longitudinal voltage in a logarithmic scale to highlight the increase of this quantity which is very small in the prebreakdown regime. We clearly observe the exponential increase of the longitudinal conductivity with the current amplitude, which was reported several times by different authors[7,20,26–28] and refered to as the prebreakdown regime. The exponential increase of V_{xx} begins with the onset of dissipation for V_c. When V_{xx} reaches the abrupt onset of dissipation (the breakdown), V_c begins to decrease. This demonstrates that there exists a strong correlation between

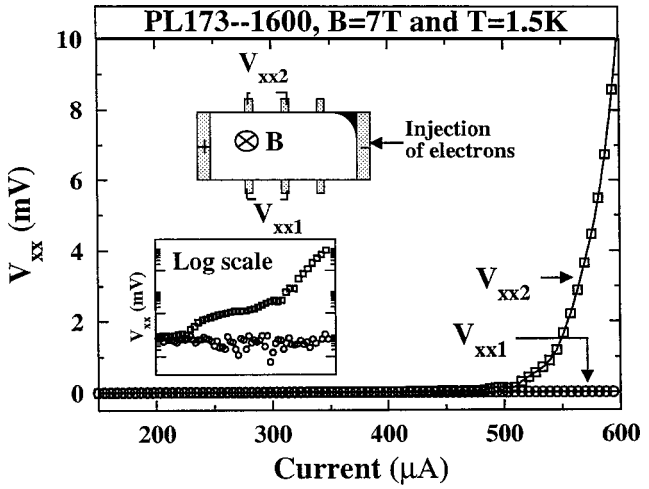

FIG. 5. Measurement of two longitudinal voltages V_{xx1} and V_{xx2} for sample PL173 with width Hall bar 1600 μm and for $B=7$ T. V_{xx2} is measured on the same side of the additional heated region along the electron flow. In the inset, the same graph in log scale highlights the huge difference in the behavior of each side of the sample (an offset has been added to V_{xx1}, the current scale is the same than in the figure).

the voltage drop across the contact and the usual longitudinal voltage drop V_{xx}.

We have also compared the longitudinal voltage V_{xx1} and V_{xx2} measured simultaneously on lower and upper side of the sample (see Fig. 5). The voltage drop measured on the same side of the ''heated region'' (V_{xx2} in the inset) increases before the one measured on the other side (V_{xx1} in the inset). This observation has been made for all samples. In the wide samples (800 and 1600 μm), the differences between V_{xx1} and V_{xx2} were huge. In the case of the narrower sample (200 μm) the discrepancies were small but still clearly observable.

We conclude that the heating process near the contact governs the transport mechanism along the electron paths. Therefore, our experimental protocol allows one to detect the slightest increase of the longitudinal voltage, by measuring the voltage drop across the contact.

C. Configurations for measurements and experimental procedure

Reversing the current polarity and the magnetic field, one obtains four different configurations which are shown in Fig. 6. Indeed if the current is reversed, then the electrons enter the opposite side of the Hall bar and the direction of the magnetic field determines where the hot spots appear. For all samples we studied the four configurations systematically.

For each configuration 1, 2, 3, and 4 of Fig. 6, our experimental procedure is as follows. The $V_c(I)$ and $V_{xx}(I)$ characteristics are measured for a whole range of magnetic field around the filling factor $\nu=2$. As an example, Fig. 7 shows $V_c(I)$ and $V_{xx}(I)$ at different filling factors. We define the current threshold of one of these curves as the current for which the voltage reaches the value of 50 μV. It can be seen from Fig. 7 that the current threshold reaches a maximum value at a well-defined value of the filling factor ν. Therefore, we can define I_c and I_b, respectively, as being the maximum value for the $V_c(I)$ and $V_{xx}(I)$ current thresholds.

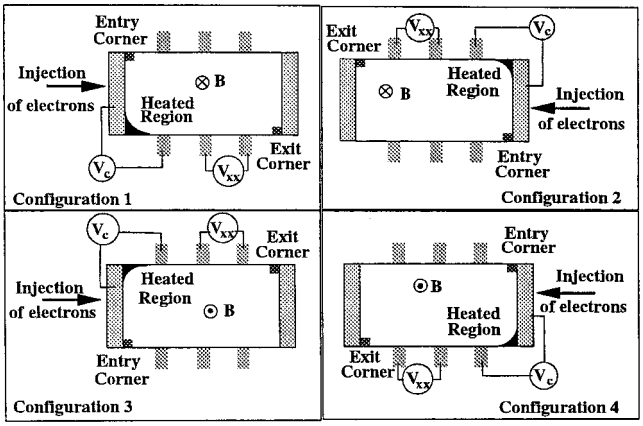

FIG. 6. Four configurations can be used to measure the contact voltage drop V_c and the longitudinal voltage drop V_{xx}. These configurations are determined by the direction of the current and of the magnetic field.

Finally, for a given configuration, one gets the value of I_b and I_c. While determining these currents, V_{xx} was kept below the onset of dissipation. In this manner, we have clearly observed, while sweeping up and down the magnetic field (Fig. 7), that the curves were reproducible. Indeed, the reproducibility of the $V_c(I)$ and $V_{xx}(I)$ curves is not satisfied anymore if the current is increased up to the breakdown.[24,29]

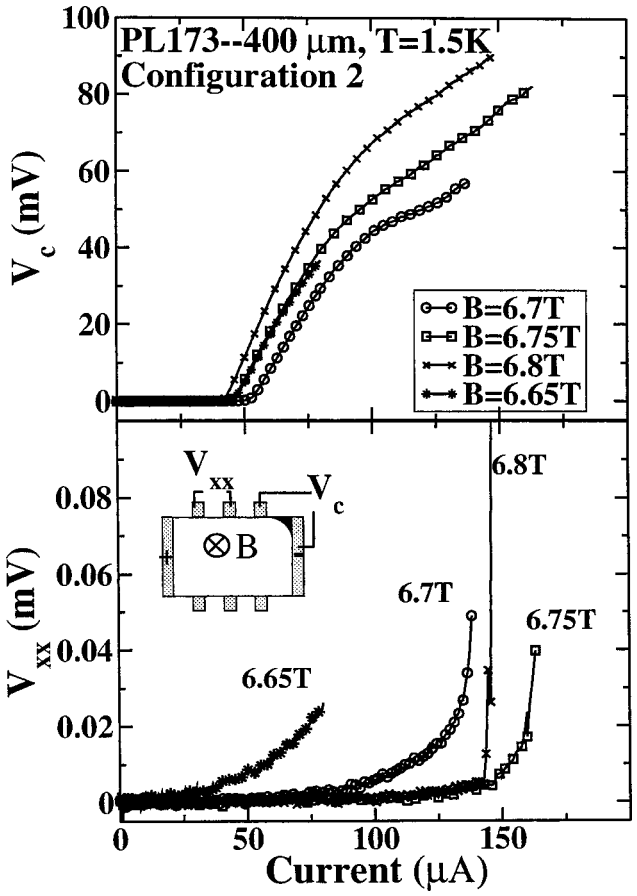

FIG. 7. Current dependence of V_{xx} and V_c for different magnetic fields around $\nu=2$.

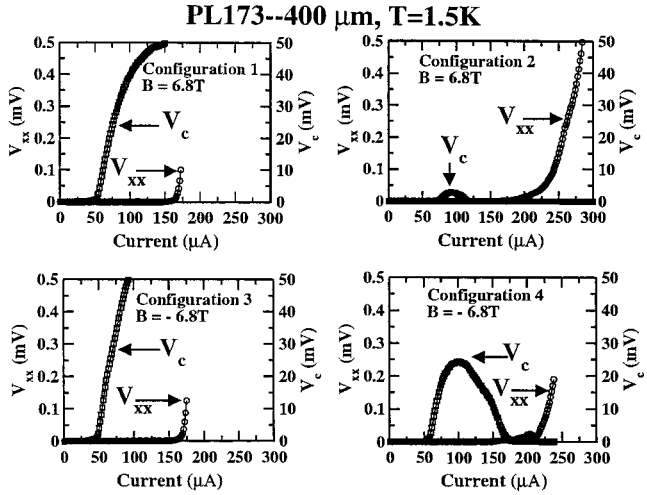

FIG. 8. Measurement of $V_{xx}(I)$ ("○") and $V_c(I)$ ("□") for sample PL173 with Hall bar width 400 μm in the four configurations. These curves correspond to the magnetic field which gives the maximum values for I_b and I_c. The critical current for V_c is much lower than the critical current for V_{xx}. Configuration 1 (respectively, 2) is similar of the configuration 3 (respectively, 4).

Several magnetic field values were investigated, allowing a precise and reproducible measurement of the critical currents I_c and I_b for each configuration.

IV. PERFORMANCES OF THE CONTACTS

A. Variation of the threshold current with the width of the contact

In this part, we present the results obtained for the PL173 and PL175 series. We have measured the critical currents I_c and I_b for each sample in all configurations following the experimental procedure described above. Before discussing and comparing the results for both series of samples, we present, as an example, the results obtained for the four configurations of the PL173-400 sample. Figure 8 shows the $V_c(I)$ and $V_{xx}(I)$ characteristics allowing the determination of I_c and I_b for this sample. Each quadrant of Fig. 8 corresponds to one of the four configurations given in Fig. 6.

We must first notice that I_c is systematically lower than I_b. The second noticeable point is the strong similarity between configurations 1 and 3 and configurations 2 and 4. This is because in configurations 1 and 3 electrons are injected by the same current contact. In configurations 2 and 4 electrons are injected by the other one. We found that every contact of each sample had its own signature. As a consequence, we took the mean value of the critical currents obtained in configurations 1 and 3 (respectively, 2 and 4) to characterize one contact (respectively, the other contact). We proceeded differently for the threshold current I_b because the measurement of V_{xx} involves different pairs of lateral contacts in the sample. We charaterize I_b with four different values corresponding to the four configurations.

By these means, we could address the graphs of the dependence of the critical currents on the channel width for the PL173 and PL175 samples.

Figure 9 is devoted to the critical current I_c for the onset

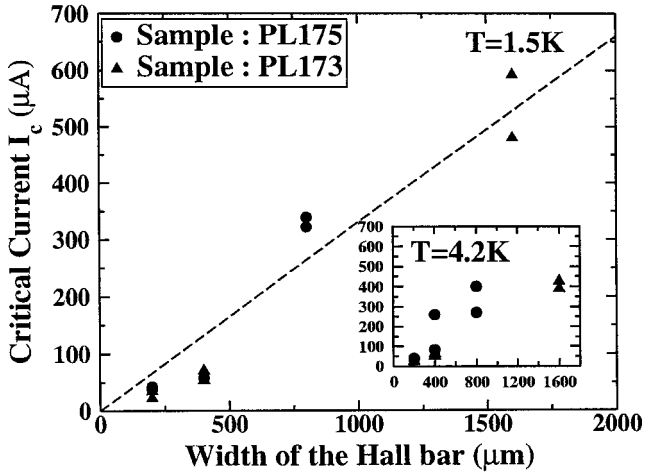

FIG. 9. The critical current I_c of the contact resistance as a function of the width of the current contact (Hall bar). The dashed line is the linear fit $I_c = 0.33 \times W$.

of the voltage drop across the contact. We observe clearly that this critical current increases with the width of the contact. This increase is linear for both PL173 and PL175 samples. The mean current density deduced from the data is $J_{cr} = 0.33$ A/m. There are no other results in the litterature which concerns the threshold current for the onset of V_c. All results concerning critical currents refer to the breakdown of the quantum Hall effect, which is a different physical phenomenon as previously explained.[16,30] In the literature, for standard Hall bars, critical current densities for the breakdown of the QHE range from $J_{cr} = 0.5$ A/m to $J_{cr} = 1.6$ A/m.[6,7,20,26,31–33] The critical current density measured here for the onset of V_c, is lower than those values. Our result confirms the difference between this phenomenon and the breakdown of the QHE.

We focus now on the general increase of I_b with the width W. In Fig. 10 the values of I_b have been plotted as a function of the width W. There are four points for one sample. In this graph we clearly remark an important dispersion of the different points which characterize one sample.

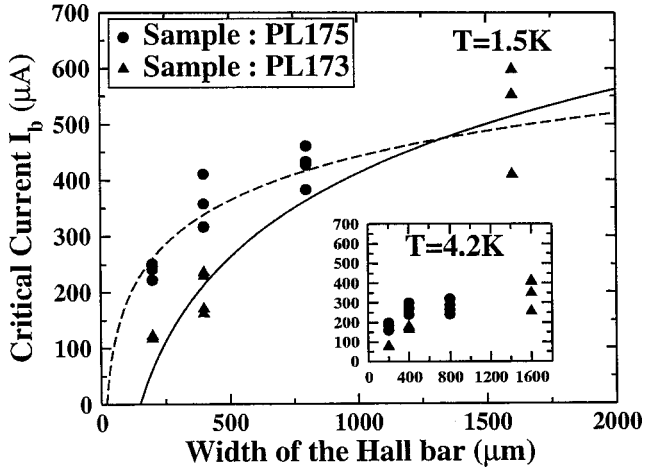

FIG. 10. The critical currents I_b of V_{xx} as a function of the Hall bar width. Each point corresponds to one configuration for each sample. Dashed line is the log fit: $I = 500 \log(W/150)$. Full line is the log fit: $I = 260 \log(W/25)$.

Again, this is an argument to stress that the configuration of the measurement is of primary importance when studying the heating effect in large Hall bars. The monotonic increase of I_b is not obviously linear like that of I_c. Indeed we could fit the results for I_b with the law $I_{cr}=I_0\log(W/W_0)$ stated by Balaban *et al.*[34] As shown in Fig. 10, the data for PL175 correspond to the curve $I=500\log(W/150)$ while the data for PL173 are fitted with $I=260\log(W/25)$. A sublinear increase for I_b is not in contradiction with other works because the mobilities for the PL173 and 175 samples are quite high (see Table I). In most samples studied in the literature the general tendancy for the breakdown current is a linear dependence $I_b(W)$. Kawaji *et al.*[32] and Okuno *et al.*[33] have already observed that the critical current of the breakdown I_b increases linearly as a function of the Hall bar width. Also Boisen *et al.*[27] observed a linear increase of I_b. This law has only one exception which was reported by Balaban *et al.*[34] who observed a sublinear increase of the critical current in very clean samples whose mobility is $\mu=90\ \mathrm{m^2/V\,s}$. In another paper, Balaban Meirav and Shtrikman[35] remarked that an intermediate mobility sample ($\mu=12\ \mathrm{m^2/V\,s}$) could exhibit both a linear increase in the dark and a sublinear increase under illumination.

Concerning our data, we can notice that the region of the contacts is undoubtly less perfect than the inner sample because of the inhomogeneities of the density caused by the presence of the ohmic contact. This can explain why $I_c(W)$ exhibits a linear increase, while $I_b(W)$ seems to fit with a sublinear increase.

We add two remarks. One concerns the fact that the critical currents for the PL173 samples are always lower than those for the PL175 samples. We attribute this difference to the magnetic field at which the experiments are performed ($B=9$ T for PL175, instead of $B=6.8$ T for PL173). Indeed, it was shown by Kawaji *et al.*[32] and also by Jeckelmann *et al.*[36] that the critical current of the longitudinal voltage scales with the magnetic field as $I_b\propto B^{3/2}$. This dependence is generally understood in terms of inter-Landau level transitions.[32,37–42]

The second remark concerns the evolution of I_b and I_c with the temperature. In both graphs in Figs. 9 and 10, the insets report the same measurements at the liquid helium temperature ($T=4.2$ K). First, these measurements confirm the measurements at 1.5 K because the graphs are similar at first sight. Second, the modifications induced by a cooling of the system are clearly observable: Most critical currents measured at 4.2 K are lower than those measured at 1.5 K. This increase of the critical current while lowering the temperature has been precisely studied by L. B. Rigal *et al.*,[43] although this was not for the critical current of the voltage drop across the contact.[44]

B. What is a good contact?

We compare now the results obtained for the critical currents of the PL173, PL174, and PL175 samples to the critical currents of sample LEP514. In order to compare the results with those of LEP514 whose channel width is 400 μm, we will only consider PL173-400 and PL175-400. Besides, we can also make a comparison between LEP514 and PL174 ($W=400\ \mu$m, $d=50\ \mu$m), both a which have exactly the same geometry (see Table I). Using the current contact as a source, we measured the values of the critical currents I_c and I_b for LEP514 and PL174-50. We reported in Table II, the mean value for the critical currents obtained for both contacts of each sample.

TABLE II. Critical currents for the 400 μm wide current contacts.

Sample	PL173	PL175	PL174	LEP514
I_c	75	70	120	440
I_b	200	350	350	570

The differences between LEP514 and the other three PL samples are remarkable. First, the series PL always exhibit a much lower value for I_c than for I_b. This is not the case for LEP514. Second, for LEP514, the high values of these critical currents (around 500 μA) are much higher than the values for the PL series (see Table II). In Fig. 11, we present the curves $V_c(I)$ and $V_{xx}(I)$ for one configuration of LEP514 which allows one to observe that the critical current of V_c is equivalent to the critical current of V_{xx}. This figure must be compared to Fig. 8. It is obvious that this sample behaves in a better manner than the PL series when the current is increased. Therefore, we conclude that LEP514 allows very accurate metrological measurements[11] because of the quality of its contacts. A good contact is robust against the formation of an extended high electric field zone in its vicinity, when the current is increased.

V. PERSPECTIVES

Throughout our experiments the PL samples exhibit a different behavior than LEP514: For PL samples of a width of 400 μm the critical currents I_c were much lower than I_b, while in the case of LEP514, the critical current I_c and I_b were nearly the same. This demonstrates that the region of high electric field near the source can have a different shape and dimension according to the sample or to the contact characteristics. At low current intensity, the high electric field

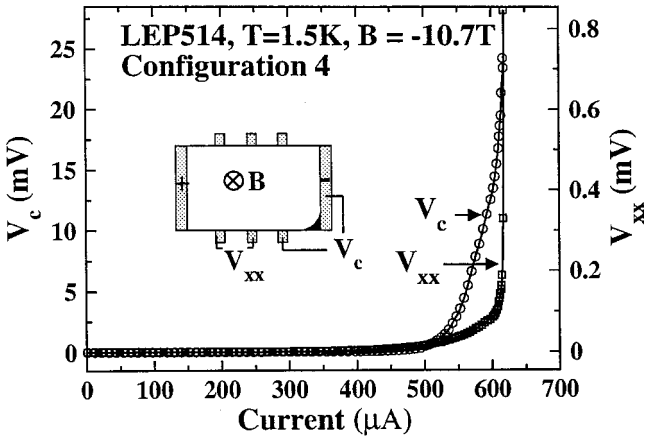

FIG. 11. Measure of $V_c(I)$ and $V_{xx}(I)$ for sample LEP514 at $i=2$ plateau for $B=10.7$ T in configuration 4.

zone is restricted to the hot spots. Let us stress that the hot spot size increases drastically with the current amplitude in the prebreakdown regime. First, the hot spot extends to the whole source side of the Hall bar. At even higher currents, it extends toward the drain side by following the electron flow. As a consequence, if the current is high enough, the contact used to measure V_c is connected to a high electric field region. This extension has undoubtedly a different shape and dimension in different samples. For instance, in the case of LEP514, the extension is smaller than in the case of the PL samples. The quality of the contacts certainly influences the formation and the extension of the high field domain, but we have shown that the size of the contact is a determining factor.

Consequently, we stress that the contact size should be maximized in the design of samples for metrological use. If one wants to keep constant the width of the channel, it might still be possible to design a jagged contact line, with crenels, in order to increase the final length of the contact.

Besides, it is clear that the experimental protocol we have proposed might be very useful for all experiments on the breakdown of the quantum Hall effect.

VI. CONCLUSION

We have demonstrated that the influence of the configuration is of great importance for high precision measurements. Thus a new measurement protocol has been used to characterize properly the pre-breakdown regime of the QHE. We have characterized for the first time the voltage drop across the contact and dressed the graph of the variation for its critical current with the width of the channel. We concluded that the contact width should be increased to optimize the injection phenomenon in the inner two dimensional electron gaz. This could help metrologists to make their measurements with a greater current, and consequently to improve their measurement. We proposed as well, that V_c should be measured while observing the breakdown phenomenon in any kind of samples, in order to control the raise of the electronic temperature.

ACKNOWLEDGMENT

This work was performed under a grant from the Bureau National de Métrologie.

[1] K. von Klitzing, G. Dorda, and M. Pepper, Phys. Rev. Lett. **45**, 494 (1980).
[2] *The Quantum Hall Effect*, edited by R. E. Prange and S. M. Girvin (Springer, New York, 1987).
[3] D. C. Tsui, H. L. Stormer, and A. C. Gossard, Phys. Rev. Lett. **48**, 1559 (1982).
[4] J. L. Robert, A. Raymond, J. Y. Mulot, C. Bousquet, W. Zawadzki, M. Kubisa, and J. P. André, Phys. Rev. B **39**, 1832 (1989).
[5] *Comité International des Poids et Mesures (CIPM), Recommandation of (BIPM, Sèvres, 1988) and Recommendation of (CCEM-2000), 22nd Sessions* (BIPM, Sèvres, 2000).
[6] G. Nachtwei, Physica E (Amsterdam) **4**, 79 (1999).
[7] B. Jeckelmann and B. Jeanneret, Rep. Prog. Phys. **64**, 1603 (2001).
[8] F. Piquemal, Bulletin du BNM **116**, 2 (1999).
[9] M. E. Cage, B. F. Field, R. F. Dziuba, S. M. Girvin, A. C. Gossard, and D. C. Tsui, Phys. Rev. B **30**, 2286 (1984).
[10] W. Poirier, A. Bounouh, K. Hayashi, H. Fhima, F. Piquemal, G. Geneves, and J. P. André, J. Appl. Phys. **92**, 2844 (2002).
[11] F. Piquemal, G. Geneves, F. Delahaye, J. P. André, J. N. Patillon, and P. Frijlink, IEEE Trans. Instrum. Meas. **42**, 264 (1993).
[12] U. Klass, W. Dietsche, K. von Klitzing, and K. Ploog, Z. Phys. B: Condens. Matter **82**, 351 (1991).
[13] P. C. van Son, G. H. Kruithof, and T. M. Klapwijk, Phys. Rev. B **42**, 11 267 (1990).
[14] P. C. van Son, G. H. Kruithof, and T. M. Klapwijk, Surf. Sci. **229**, 57 (1990).
[15] Y. Kawano and S. Komiyama, Phys. Rev. B **61**, 2931 (2000).
[16] C. Chaubet, Y. M. Meziani, B. Jouault, A. Raymond, W. Poirier, and F. Piquemal, Semicond. Sci. Technol. **18**, 983 (2003).
[17] C. Chaubet, A. Raymond, and D. Dur, Phys. Rev. B **52**, 11 178 (1995).
[18] C. Chaubet and F. Geniet, Phys. Rev. B **58**, 13 015 (1998).
[19] Y. Kawano, Y. Hisanaga, and S. Komiyama, Phys. Rev. B **59**, 12 537 (1999).
[20] S. Komiyama, T. Takamasu, S. Hiyamizu, and S. Sasa, Solid State Commun. **54**, 479 (1985).
[21] Y. Kawaguchi, F. Hayashi, S. Komiyama, T. Osada, Y. Shiraki, and R. Itoh, Jpn. J. Appl. Phys., Part 1 **34**, 4309 (1995).
[22] S. Komiyama, Y. Kawaguchi, T. Osada, and Y. Shiraki, Phys. Rev. Lett. **77**, 558 (1996).
[23] S. Komiyama and Y. Kawaguchi, Phys. Rev. B **61**, 2014 (2000).
[24] G. Boella, L. Cordiali, G. Marullo-Reedtz, D. Allasia, G. Rinaudo, M. Truccato, and C. Villavecchia, Phys. Rev. B **50**, 7608 (1994).
[25] B. E. Sagol, G. Nachtwei, K. von Klitzing, G. Hein, and K. Eberl, Phys. Rev. B **66**, 075305 (2002).
[26] G. Ebert, K. Von Klitzing, K. Ploog, and G. Weimann, J. Phys. C **16**, 5441 (1983).
[27] A. Boisen, P. Boggild, A. Kristensen, and P. E. Lindelof, Phys. Rev. B **50**, 1957 (1994).
[28] M. Furlan, Phys. Rev. B **57**, 14 818 (1998).
[29] F. J. Ahlers, G. Hein, H. Scherer, L. Bliek, H. Nickel, R. Losch, and W. Schlapp, Semicond. Sci. Technol. **8**, 2062 (1990).
[30] Y. M. Meziani, C. Chaubet, B. Jouault, S. Bonifacie, A. Raymond, W. Poirier, and F. Piquemal, Physica B, in press, Corrected Proof, Available online 8 March, 2004.
[31] M. E. Cage, R. F. Dziuba, B. F. Field, E. R. Williams, S. M. Girvin, A. C. Gossard, D. C. Tsui, and R. J. Wagner, Phys. Rev. Lett. **51**, 1374 (1983).
[32] S. Kawaji, K. Hirakawa, N. Nagata, T. Okamoto, T. Fukasi, and T. Gotoh, J. Phys. Soc. Jpn. **63**, 2303 (1994).
[33] T. Okuno, S. Kawaji, T. Ohrui, T. Okamoto, Y. Kurata, and J. Sakai, J. Phys. Soc. Jpn. **64**, 1881 (1995).
[34] N. Q. Balaban, U. Meirav, H. Shtrikman, and Y. Levinson, Phys. Rev. Lett. **71**, 1443 (1993).
[35] N. Q. Balaban, U. Meirav, and H. Shtrikman, Phys. Rev. B **52**, 5503 (1995).
[36] B. Jeckelmann, A. Rufenacht, B. Jeanneret, F. Overney, K. Pierz, A. von Campenhausen, and G. Hein, IEEE Trans. Instrum. Meas. **50**, 218 (2001).
[37] O. Heinonen, P. L. Taylor, and S. M. Girvin, Phys. Rev. B **30**, 3016 (1984).
[38] P. S. S. Guimaraes, L. Eaves, F. W. Sheard, J. C. Portal, and G. Hill, Physica B **134**, 47 (1985).
[39] L. Bliek, E. Braum, G. Hein, V. Kose, J. Niemeyer, G. Weimann, and W. Schlapp, Semicond. Sci. Technol. **1**, 110 (1986).
[40] J. R. Kirtley, Z. Schlesinger, T. N. Theis, F. P. Milliken, S. L. Wright, and L. F. Palmateer, Phys. Rev. B **34**, 1384 (1986).
[41] L. Bliek, G. Hein, D. Jucknishke, V. Kose, J. Niemeyer, G. Weimann, and W. Sclapp, Surf. Sci. **196**, 156 (1988).
[42] L. Eaves and F. W. Sheard, Semicond. Sci. Technol. **1**, 346 (1986).
[43] L. B. Rigal, D. K. Maude, M. Potemski, J. C. Portal, L. Eaves, J. R. Wasilewski, G. Hill, and M. A. Pate, Phys. Rev. Lett. **82**, 1249 (1999).
[44] A. A. Shashkin, A. J. Kent, P. A. Harrison, L. Eaves, and M. Henini, Phys. Rev. B **49**, 5379 (1994).